Gait Event Detection from Accelerometry using the Teager-Kaiser Energy Operator

Matthew W. Flood, Ben P.F. O'Callaghan, and Madeleine M. Lowery, *Member, IEEE*

***Abstract*—*Objective*: A novel method based on the application of the Teager-Kaiser Energy Operator is presented to estimate instances of initial contact (IC) and final contact (FC) from accelerometry during gait. The performance of the proposed method was evaluated against four existing gait event detection (GED) methods under three walking conditions designed to capture the variance of gait in real-world environments. *Methods:* A symmetric discrete approximation of the Teager-Kaiser energy operator was used to capture simultaneous amplitude and frequency modulations of the shank acceleration signal at IC and FC during flat treadmill walking, inclined treadmill walking, and flat indoor walking. Accuracy of estimated gait events were determined relative to gait events detected using force-sensitive resistors. The performance of the proposed algorithm was assessed against four established methods by comparing mean-absolute error, sensitivity, precision and F1-score values. *Results:* The proposed method demonstrated high accuracy for GED in all walking conditions, yielding higher F1-scores (IC: >0.98, FC: >0.9) and lower mean-absolute errors (IC: <0.018s, FC: <0.039s) than other methods examined. Estimated ICs from shank-based methods tended to exhibit unimodal distributions preceding the force-sensitive resistor estimated ICs, whereas estimated gait events for waist-based methods had quasi-uniform random distributions and lower accuracy. *Conclusion:* Compared to established gait event detection methods, the proposed method yielded comparably high accuracy for IC detection, and was more accurate than all other methods examined for FC detection. *Significance:* The results support the use of the Teager-Kaiser Energy Operator for accurate automated GED across a range of walking conditions.**

***Index Terms*—Accelerometry, Final Contact, Gait Event Detection, Initial Contact, Teager-Kaiser Energy Operator, Treadmill Walking, Shank Mounted, Waist Mounted**

I. Introduction

THE advent of low-cost inertial measurement units has been central to the rapidly developing field of wearable technology for gait analysis [1], [2]. Temporal parameters of the gait cycle have been used to analyse human locomotion in a variety of medical conditions including Parkinson's disease [3]–[5], knee osteoarthritis [6], [7], and following trans-femoral amputation [8], [9]. In many of these studies, gait cycle parameters such as step time, swing/stance duration and step asymmetry have been shown to capture subtle progressive changes that occur in gait with rehabilitation or disease [4]–[7]. To evaluate such parameters, detection of two key events of the gait cycle are required - initial contact (IC) and final contact (FC) [10]. The proliferation of studies using accelerometry (ACC) for gait analysis has been accompanied by an increasing number of methodologies seeking to detect IC and FC events as accurately as possible [11]–[17]. The performance of these gait event detection (GED) algorithms can vary greatly depending on sensor location, computational approach, and cadence [10], [18], [19]. Furthermore, not all methods provide a means for FC detection [16], [20], [21], limiting the number of temporal gait parameters which can be derived.

To improve FC detection, it has been suggested that shank-mounted ACC may provide more signal information which could be used to identify instances of FC [19]. The choice of sensor location is an important factor to consider in study design with regard to ease of application, subject compliance and the range activities that can be detected [22], [23]. For monitoring tasks of daily living, waist mounted accelerometers placed near the centre of mass are often preferable as sensor positioning is relatively simple and energy expenditure from several activities can be estimated with a single sensor [22]–[24]. However, comparative studies have shown that waist mounted sensors perform worse than shank mounted sensors for detecting ICs and FCs [10], [19], potentially influencing the accuracy of temporal gait cycle parameters obtained in situations where gait variability is increased. As shank mounted accelerometers are closer to the point of IC and FC, they may intrinsically capture information integrated in the ACC signal that could be absent when recorded at the waist [19].

The computational approach most commonly adopted for GED involves digital filtering in conjunction with zero-crossing and/or peak detection [13]–[17], [20], [21]. These methods, although straightforward to implement, often rely on the signal having a specific profile and very precise sensor placement to perform reliably [12]. To identify gait events from ACC data when signal profiles may be inconsistent, recent studies have applied the continuous wavelet transform (CWT), capitalizing on its localised time-frequency properties [11], [12]. Many of the available GED methods imply a number of *a priori* assumptions about the data such as subject cadence or gait regularity [12]. For ambulatory monitoring in a real-world environment, automated algorithms must be robust enough to accurately extract ICs and FCs across a range of conditions, where some of these assumptions may not apply, or where linear filtering techniques may be inadequate [25]. Ideally, a GED algorithm should also be computationally efficient to

This work is supported in part by Science Foundation Ireland under grant number SFI/12/RC/2289 and the European Research Council under the grant number ERC-2014-CoG-646923. *(Corresponding Author: Matthew Flood)*

M. W. Flood, B. P.F. O'Callaghan, and M. M. Lowery are with the Neuromuscular Systems Research Group, School of Electrical & Electronic Engineering, University College Dublin, Belfield, Dublin 4, Ireland. (e-mail: matthew.flood@ucdconnect.ie;)

M. W. Flood and M. M. Lowery are also with the Insight Centre for Data Analytics, O'Brien Centre for Science, at University College Dublin, Belfield, Dublin 4, Ireland.

enable online feedback in real time.

To achieve high accuracy with computational efficiency while minimizing *a priori* assumptions, the present manuscript proposes a novel algorithm that utilizes the Teager-Kaiser Energy Operator (TKO) to identify instances of IC and FC during gait from ACC recorded at the shank. The TKO is based on the phenomenological model proposed by Teager and Teager to estimate the energy of a speech signal [26], [27]. Teager and Teager argued that conventional linear filtering techniques based on Fourier theory were insufficient to accurately analyse speech due to the nonlinear processes in the vocal tract. Later mathematically derived by Kaiser [28], the TKO has since been used to detect features of a variety of signals, from electromyography [29] to sperm whale clicks [30], and briefly in the estimation of stride length using ACC [31]. Here we propose the TKO as a reliable method for identifying the simultaneous changes in amplitude and frequency of the acceleration signal that occur at the points of IC and FC. This paper presents the first application of the TKO to detect localised, high-frequency changes in ACC signals that occur at IC and FC events during gait.

The performance of the proposed TKO method for gait event detection, henceforth referred to as TK_{GED}, was compared with four other algorithms - two designed for waist mounted sensors [11], [13], and two designed for shank mounted sensors [3], [12]. For each sensor position, one chosen method used digital filtering with peak detection [3], [13], and the other used the CWT [11], [12]. TK_{GED} demonstrated high accuracy for IC and FC detection across a variety of walking conditions typical of tasks in daily living. Accuracy was comparable to the best of the shank-based methods for IC detection, and higher than that of all other methods examined for FC detection.

II. Methods

A. TK_{GED} Procedure:

The basic Teager-Kaiser Energy Operator is defined as,

$$\psi\,[x(t)] = \dot{x}^2(t) - x(t)\ddot{x}(t) \tag{1}$$

where $\psi[x(t)]$ represents the estimated energy of the signal x at time t, and $\dot{x}$ and $\ddot{x}$ represent the first and second derivatives of x respectively. Translating (1) to the discrete time case requires approximating $\dot{x}(t)$ using either a two-sample backward difference (2) or a two-sample forward difference method (3) [32],

$$\psi\,[x(t)] \;\mapsto\; \left(x_{n-1}^2 - x_n x_{n-2}\right)\Big/ T_s^2 \tag{2}$$

$$\psi\,[x(t)] \;\mapsto\; \left(x_{n+1}^2 - x_n x_{n+2}\right)\Big/ T_s^2 \tag{3}$$

where T_S is the sampling period, n is the sample number, and $\mapsto$ denotes the mapping from continuous time to discrete time.

For both translations of $\psi[x(t)]$ in (2) and (3) the resulting approximation is asymmetric. To obtain a symmetric discrete form of $\psi[x(t)]$, a three-sample symmetric difference is calculated by averaging the first and second derivative approximations,

$$\dot{x}(t) \mapsto \left[(x_{n+1} - x_n) + (x_n - x_{n-1})\right]\Big/ 2T_s$$

$$\mapsto \left(x_{n+1} - x_{n-1}\right)\Big/ 2T_s \tag{4}$$

$$\ddot{x}(t) \mapsto \left\{\begin{matrix}[(x_{n+2} - x_n) - (x_{n+1} - x_{n-1})] \\ +\,[(x_{n+1} - x_{n-1}) - (x_n - x_{n-2})]\end{matrix}\right\}\Big/ 4T_s^2$$

$$\mapsto \left(x_{n+2} - 2x_n + x_{n-2}\right)\Big/ 4T_s^2 \tag{5}$$

$$\psi\,[x(t)] \mapsto \left[\left(x_{n+1} - x_{n-1}\right)\Big/ 2T_s\right]^2 - \left[\,x_n\left(x_{n+2} - 2x_n + x_{n-2}\right)\Big/ 4T_s^2\right]$$

Hence,

$$\varphi_n = \left[\,2{x_n}^2 + (x_{n+1} - x_{n-1})^2 - x_n(x_{n+2} + x_{n-2})\right]\Big/ 4T_s^2 \tag{6}$$

where φ_n is a symmetric discrete time estimate of the Teager-Kaiser energy. Thus, φ captures localised simultaneous increases in amplitude and frequency of the ACC signal, such as those that occur when the heel makes contact with the ground at IC and the foot leaves the ground at FC. Taking x_n to be the acceleration of the shank as recorded in the anterio-posterior direction (Fig. 1a), φ, is used to identify ICs as follows:

1) Two samples equal to φ_1 are concatenated to the start of the signal to eliminate the sample shift inherent in (6).
2) The estimated energy signal is half-wave rectified (Fig. 1b),
$$\varphi_n < 0 = 0 \tag{7}$$
3) A three sample moving maximum window is applied to φ, followed by a five sample moving average window to smooth peaks occurring within close proximity of each other (Fig. 1b),
$$\varphi'_n = \max(\varphi_{n-1},\ \varphi_n,\ \varphi_{n+1}) \tag{8}$$
$$\varphi''_n = \tfrac{1}{5}\textstyle\sum_{n-2}^{n+2}\varphi'_n \tag{9}$$
4) A peak detection method is used to identify a set of local maxima that fulfil two constraints. Constraint 1: Local maxima must be greater than a specified amplitude threshold. For the present

study, a threshold corresponding to half the mean of φ'' was used for each walking task. Constraint 2: Local maxima observing constraint 1 must be separated by a specified temporal threshold. For the present study, the temporal threshold for each walking task was set to 0.7τ, where τ represents the lag (samples) of the first positive local maximum in the autocovariance sequence of φ'', an approximation of the average stride time of the signal.

The set of estimated IC time points, *m*, corresponds to the local maxima which satisfy both constraints (Fig. 1b). Once ICs have been identified, the following steps are used to determine the subsequent FC times.

5) Values lying within a region corresponding to $\pm 0.3\tau$ about each IC are set equal to zero to leave only the peaks corresponding to FCs (Fig. 1c).

$$\chi_n = \begin{cases} \varphi''_n & n \notin (m-0.15\tau, \dots, m+0.15\tau) \\ 0 & n \subseteq (m-0.15\tau, \dots, m+0.15\tau) \end{cases} \quad (10)$$

6) A moving maximum window of 0.15τ samples is applied to χ, followed by a moving average window of 0.3τ samples applied to χ' (Fig. 1c), defined as follows,

$$\chi'_n = \max(\chi_{n-0.075\tau+1}, \cdots, \chi_{n+0.075\tau-1}) \quad (11)$$

$$\chi''_n = \frac{1}{0.3\tau} \sum_{n+1-0.15\tau}^{n-1+0.15\tau} \chi'_n \quad (12)$$

7) To identify FC times, a peak detection method was used to identify local maxima separated by 0.7τ samples using the same approach outlined in step 4.

Estimated FC times correspond to the local maxima satisfying this constraint (Fig. 1c).

B. Comparative Algorithm Implementation:

The performance of TK_{GED} was compared with four established GED methods [3], [11]–[13], each of which has previously demonstrated high GED accuracy in comparative assessments [12], [18], [19]. All methods were implemented in MatLab 2018a (Mathworks, USA) as outlined in the source literature [3], [11]–[13], and summarised as follows.

1) *W_{PKF} - Waist ACC with Peak Detection*

Acceleration in the vertical and anterio-posterior directions from a sensor located at the waist were pre-processed for artefact removal by subtracting the mean, 5th order median filtering, and normalizing the maximum amplitude to 1. A refined peak finding approach within localised windows was used to determine the temporal occurrence of IC and FC events [13].

2) *W_{CWT} – Waist ACC with Continuous Wavelet Transform*

Vertical acceleration recorded at the waist was smoothed through integration and differentiation by the CWT with a Gaussian wavelet. IC times were determined as the local

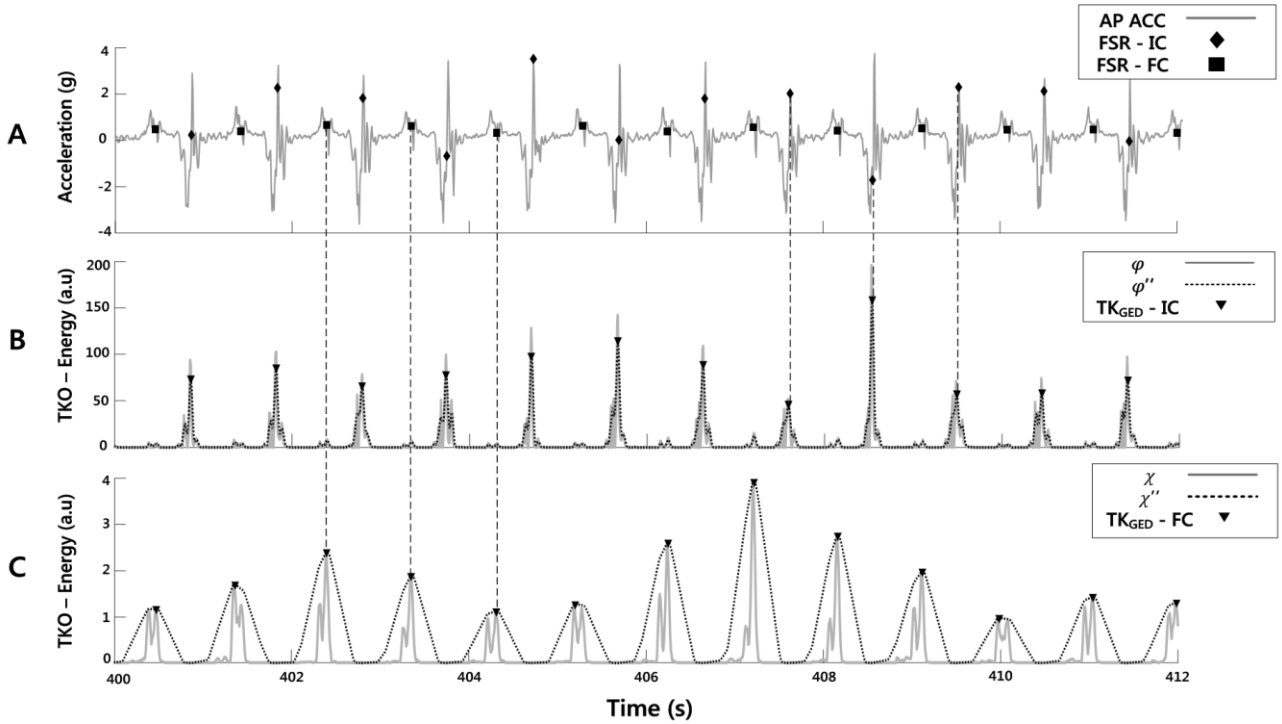

Figure 1. a) Representative raw ACC signal in the AP axis recorded at the right ankle from Subject 3 during flat treadmill walking. b) The corresponding TKO energy of the ACC signal after Steps 2 and 3. IC times are the local maxima satisfying the constraints of Step 4. c) The TKO energy signal after IC region removal and smoothing of Steps 5 and 6 . FC times are the local maxima identified in Step 7. Both TKO Energy signals in (b) and (c) are plotted with the common scaling factor $0.25 Ts^{-2}$ removed.

minima of the smoothed signal. Local maxima of the signal obtained through further differentiation by the CWT yielded FC times [11].

3) *S_{PKF} – Shank ACC with Peak Detection*

Following low frequency bias removal from the acceleration signal recorded at the ankle, a resultant magnitude signal was calculated from acceleration in each axis. The resultant magnitude signal was low pass filtered and thresholding was applied to identify periods of active walking. An adaptive windowing approach involving local peak detection was used to determine the occurrence of IC and FC events [3].

4) *S_{CWT} – Shank ACC with Continuous Wavelet Transform*

A single magnitude vector was calculated from all three axes of an accelerometer positioned at the ankle. The resulting signal undergoes a CWT with a 'morlet' wavelet and the energy at each frequency scale was estimated. Through a recursive windowing approach, gait event and gait cycle boundaries were derived from the spectral energy within each window using a bimodal Gaussian distribution approximation. IC and FC times were identified as the local maxima within each gait boundary [12].

C. Gait Dataset:

The performance of the TK_{GED} algorithm was assessed under three different walking conditions using the Movement Analysis in Real-World Environments (MAREA) dataset [33]. The MAREA dataset consists of ACC recorded from 11 healthy adults during three walking conditions – flat treadmill walking (10min), inclined treadmill walking, and indoor flat space walking. The treadmill speed in the flat walking task ranged from 4 - 8km/hr, increasing in 0.4km/hr increments every minute until a self-selected running speed was reached. Treadmill inclination angle during the inclined walking task was adjusted at 2 min intervals in the following order: 5º, 0º, 10º, 0º, 15º, 0º. Indoor flat walking was performed at the subject's self-selected speed. Each subject was equipped with a Shimmer3 tri-axial accelerometer (±8g) at the waist and both shanks, slightly above the ankle. Approximate IC and FC times were obtained from force sensitive resistors (FSR) fixed on the sole of the shoe and all data were sampled at 128 Hz. Full details are available at islab.hh.se/mediawiki/Gait_database [33].

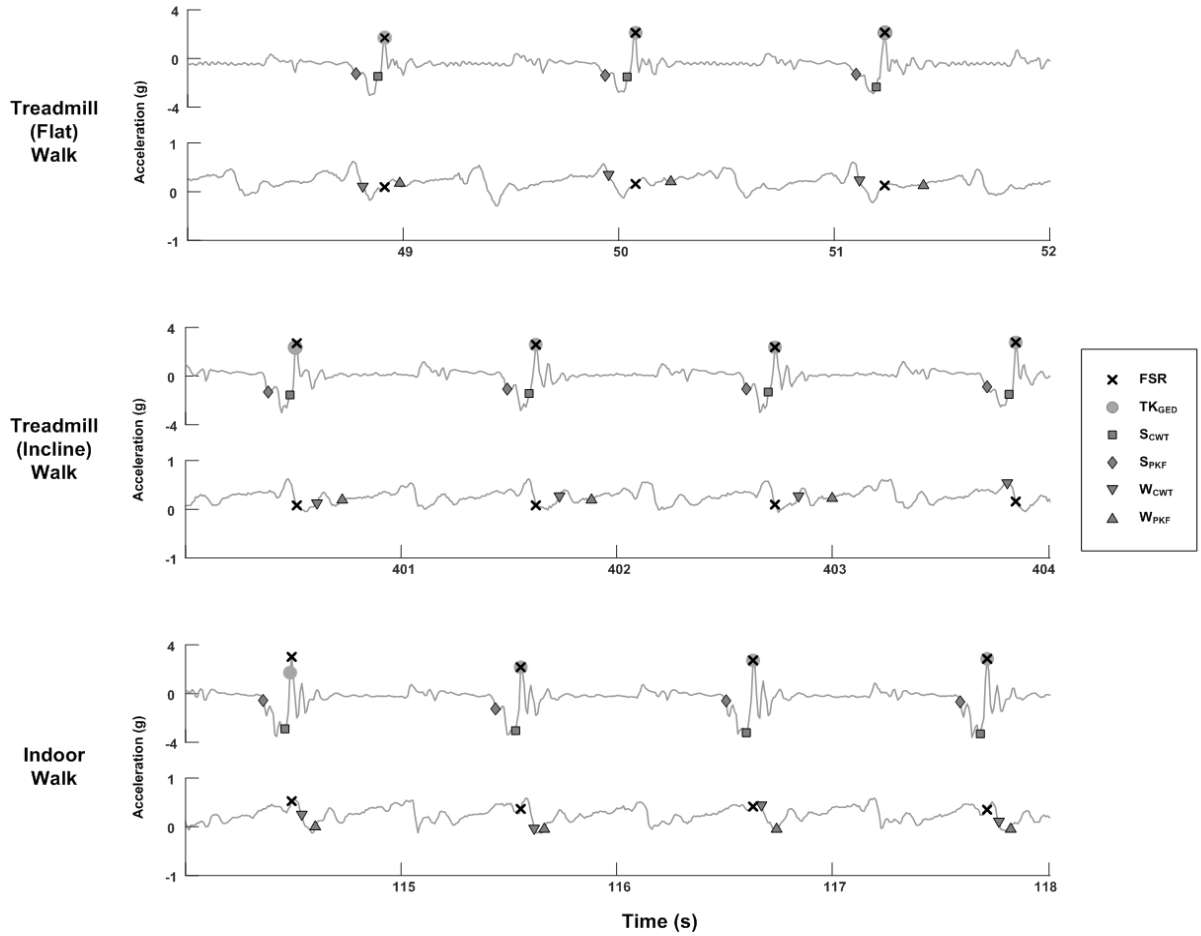

Figure 2. Representative plots comparing right leg ICs estimated for each GED method in each walking condition performed by Subject 3. For each walking condition shown, the top subplot depicts ICs estimated using shank-mounted accelerometers and the bottom subplot depicts ICs estimated using waist-mounted accelerometers. Signals for both shank and waist-based methods show acceleration in the AP direction. For the waist-based methods, only right leg IC estimates are shown and false positive ICs removed for visualisation purposes.

This article has been accepted for publication in a future issue of this journal, but has not been fully edited. Content may change prior to final publication. Citation information: DOI 10.1109/TBME.2019.2919394, IEEE Transactions on Biomedical Engineering

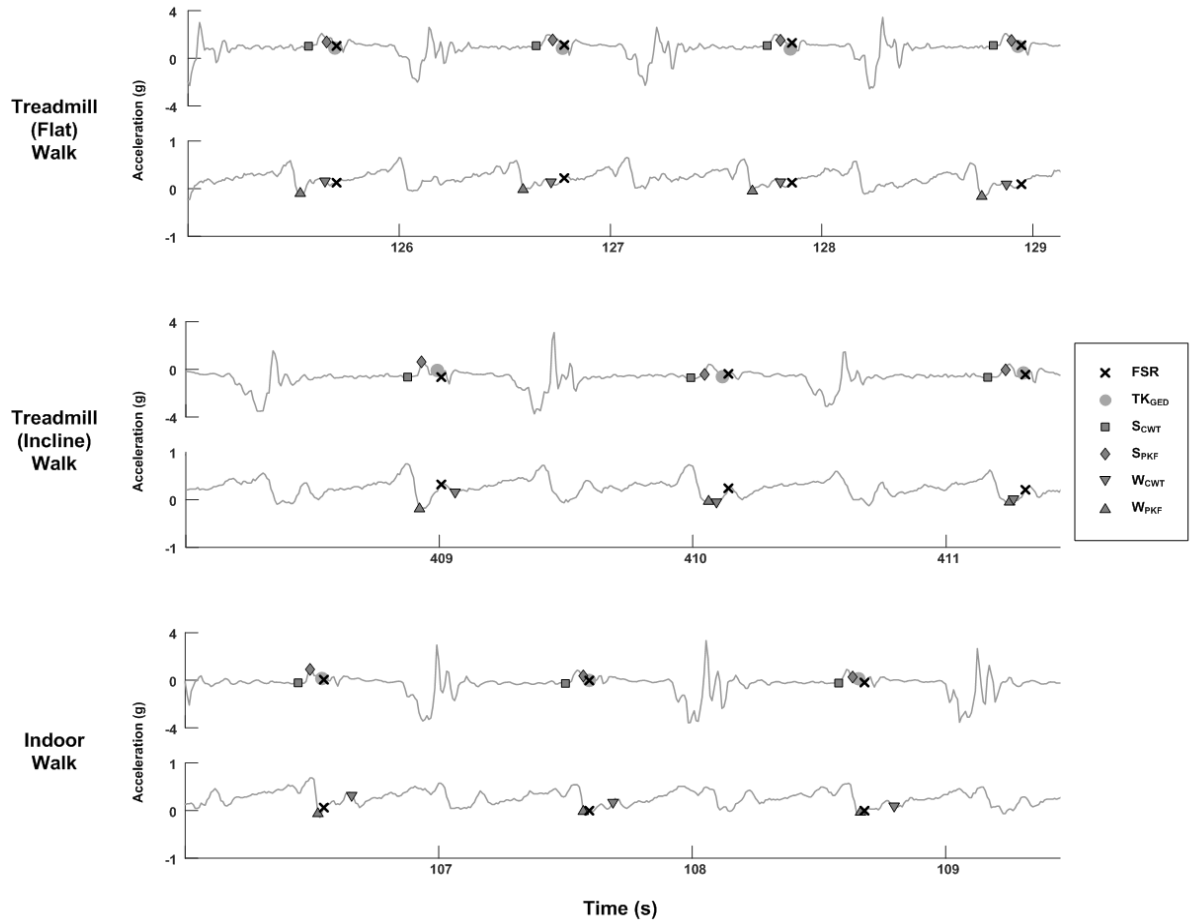

Figure 3. Representative plots comparing right leg FC estimated for each GED method in each walking condition performed by Subject 3. For each walking condition shown, the top subplot depicts FCs estimated using shank-mounted accelerometers and the bottom subplot depicts FCs estimated using waist-mounted accelerometers. Signals for both shank and waist-based methods show acceleration in the AP direction. For the waist-based methods, only right leg FC estimates are shown and false positive FCs removed for visualisation purposes.

D. Assessment of Method Accuracy:

A tolerance of ±8 samples (±0.06125s) about each FSR estimated gait event was chosen for classifying estimated gait events as true positive matches. This delay was chosen as the upper bound considered acceptable based on estimated errors reported for commonly used GED methods [19]. The total number of true and false positives was used to estimate the sensitivity (13), precision (14), and F1-score (15) for each method in all walking tasks. Sensitivity is the ratio of the number of estimated events occurring within the tolerance (# Correct Matches) to the total number of FSR gait events (# Total Possible Matches). Precision is the ratio of the number of estimated events occurring within the tolerance to the total number of gait event estimates (#Total Estimate Matches). As sensitivity and precision are often inversely correlated, the F1-score (15) combines both measures into a single weighted value calculated as the harmonic mean of sensitivity and precision [34]. If sensitivity is considered twice as important as precision, the F1-score weighting parameter, β, is assigned a value of 2. Conversely, if precision is twice as important as sensitivity, β is assigned a value of 0.5. In the present study, sensitivity and precision were considered equally important, giving β a value of 1. As described by Chincor [34], an algorithm achieving sensitivity of 50% and precision of 50% will have a higher F1-score than an algorithm that achieves sensitivity of 20% and precision of 80% (for β = 1).

$$Sensitivity = \frac{\#\ Correct\ Matches}{\#\ Total\ Possible\ Matches} \tag{13}$$

$$Precision = \frac{\#\ Correct\ Matches}{\#\ Total\ Estimate\ Matches} \tag{14}$$

$$F1 - Score = \frac{(\beta^2+1) * Sensitivity * Precision}{(\beta^2 * Sensitivity)+Precision} \tag{15}$$

The amplitude and temporal thresholds of Step 4 are chosen as scaled values of the TKO signal mean and average stride duration respectively. To assess the effect of the threshold values on the performance of TK_{GED}, sensitivity, precision and F1-score were evaluated when the proposed amplitude threshold was removed or doubled, and when the proposed temporal threshold was increased or decreased by half the average approximate stride duration. The robustness of TK_{GED}

to noise was also assessed by measuring detection accuracy following the addition of Gaussian white noise (0-60Hz) to the raw ACC data at Signal-to-Noise ratios (SNRs) ranging from 5 - 25dB in 5dB intervals.

III. Results

A. Initial Contact Detection

Table I-1 displays the mean and standard deviation of the mean absolute error, sensitivity, precision and F1-scores for IC detection in each walking task and method. Accuracy of IC estimation in each walking task was highest for the TK_{GED} and S_{CWT} methods showing consistently high sensitivity and precision values with average F1-scores > 0.98. Average F1-scores for W_{PKF}, W_{CWT}, and S_{PKF} were substantially lower, not exceeding 0.52 (Table I-1).

The distribution of accurately detected ICs relative to the FSR detected IC for each method, averaged across all subjects in each walking task is shown in Fig. 2. Estimated IC times from methods for shank mounted sensors were concentrated within the ±8 sample (0.0625s) tolerance, unlike those using methods for waist mounted sensors, which had a quasi-uniform distribution across the range of ±16 samples (0.125s). Consequently, waist-based methods showed higher mean absolute errors than shank-based methods for IC detection (Table I-1). TK_{GED} yielded the lowest mean absolute errors in each walking task (16.41ms; 17.24ms; 17.83ms), and achieved an average F1-score of 1 for all tasks when the tolerance boundaries were expanded to ±11 samples (<0.086s).

B. Final Contact Detection

The mean and standard deviation of performance scores for FC detection are displayed in Table I-2. TK_{GED} was the only method to achieve F1-scores > 0.9 for FC detection accuracy with values of 0.9, 0.98 and 0.96 for treadmill flat walking, treadmill incline walking, and indoor walking respectively (Table I-2). Similar to the results for IC detection, the performance of shank-based methods TK_{GED} and S_{PKF} ranked higher than waist-based methods for FC estimation where no F1-score >0.44 was observed. In contrast to its accuracy for IC detection, the accuracy of S_{CWT} was lower for FC detection (F1-score <0.3).

Fig. 3 presents the distribution of detected FCs within the tolerance boundaries of the FSR approximated FC for each method and walking task. Similar to IC detection, FC times of methods for shank mounted sensors had lower mean absolute errors (Table I-2) and displayed clustered distributions about the mean, whereas methods using waist mounted ACC showed uniformly distributed FC estimations and higher mean absolute errors. Unlike TK_{GED} and S_{PKF}, the majority of FC estimates for S_{CWT} were centred between 10-12 samples after the FSR approximated FC in the walking tasks, resulting in average mean absolute errors >85ms. For the incline treadmill and indoor walking tasks, TK_{GED} obtained an average F1-score of 1

Table I.
Mean (SD) of mean absolute error, sensitivity, precision, and F1-score values for estimated (1) initial contact and (2) final contact times of each method.

1

Measure:	*Method:*	Treadmill Walking (Flat)	Treadmill Walking (Incline)	Indoor Flat Walking
Mean Absolute Error (ms)	TK_{GED}	16.41 (6.61)	17.24 (9.22)	17.83 (7.38)
	W_{PKF}	100.69 (71.41)	116.37 (60.72)	140.11 (87.26)
	W_{CWT}	81.37 (61.47)	81.54 (37.89)	103.91 (75.4)
	S_{PKF}	77.02 (25.42)	82.84 (31.19)	84.45 (24.09)
	S_{CWT}	20.1 (10.12)	20.19 (4.74)	19.28 (6.86)
Sensitivity	TK_{GED}	0.99 (0.03)	0.98 (0.04)	0.99 (0.01)
	W_{PKF}	0.46 (0.35)	0.3 (0.31)	0.27 (0.32)
	W_{CWT}	0.57 (0.33)	0.43 (0.31)	0.45 (0.43)
	S_{PKF}	0.33 (0.31)	0.32 (0.29)	0.26 (0.26)
	S_{CWT}	0.97 (0.06)	0.99 (0.01)	0.99 (0)
Precision	TK_{GED}	0.99 (0.03)	0.98 (0.04)	0.99 (0.01)
	W_{PKF}	0.46 (0.35)	0.3 (0.31)	0.27 (0.32)
	W_{CWT}	0.48 (0.3)	0.32 (0.22)	0.35 (0.32)
	S_{PKF}	0.24 (0.22)	0.24 (0.21)	0.2 (0.2)
	S_{CWT}	0.98 (0.06)	0.99 (0.01)	1 (0)
F1-Score	TK_{GED}	0.99 (0.03)	0.98 (0.04)	0.99 (0.01)
	W_{PKF}	0.46 (0.35)	0.3 (0.31)	0.27 (0.32)
	W_{CWT}	0.52 (0.31)	0.36 (0.25)	0.39 (0.36)
	S_{PKF}	0.28 (0.25)	0.27 (0.24)	0.22 (0.22)
	S_{CWT}	0.98 (0.06)	0.99 (0.01)	0.99 (0)

2

Measure:	*Method:*	Treadmill Walking (Flat)	Treadmill Walking (Incline)	Indoor Flat Walking
Mean Absolute Error (ms)	TK_{GED}	39.84 (16.1)	27.45 (6.08)	26.98 (14.75)
	W_{PKF}	111.04 (52.88)	94.47 (44.78)	121.69 (75.48)
	W_{CWT}	97.61 (42.23)	87.49 (43.82)	131.2 (67.94)
	S_{PKF}	75.17 (53.71)	82.81 (43.31)	75.69 (41.18)
	S_{CWT}	85.68 (20.54)	111.94 (23.07)	106.93 (17.99)
Sensitivity	TK_{GED}	0.9 (0.15)	0.98 (0.02)	0.96 (0.11)
	W_{PKF}	0.38 (0.21)	0.44 (0.23)	0.36 (0.34)
	W_{CWT}	0.4 (0.25)	0.45 (0.26)	0.26 (0.3)
	S_{PKF}	0.72 (0.26)	0.71 (0.22)	0.73 (0.26)
	S_{CWT}	0.29 (0.18)	0.06 (0.14)	0.06 (0.13)
Precision	TK_{GED}	0.9 (0.15)	0.98 (0.02)	0.96 (0.11)
	W_{PKF}	0.39 (0.21)	0.44 (0.23)	0.36 (0.34)
	W_{CWT}	0.35 (0.24)	0.34 (0.2)	0.2 (0.23)
	S_{PKF}	0.67 (0.28)	0.64 (0.23)	0.69 (0.26)
	S_{CWT}	0.29 (0.19)	0.06 (0.14)	0.07 (0.14)
F1-Score	TK_{GED}	0.9 (0.15)	0.98 (0.02)	0.96 (0.11)
	W_{PKF}	0.39 (0.21)	0.44 (0.23)	0.36 (0.34)
	W_{CWT}	0.37 (0.24)	0.38 (0.22)	0.22 (0.26)
	S_{PKF}	0.69 (0.27)	0.67 (0.23)	0.71 (0.26)
	S_{CWT}	0.29 (0.18)	0.06 (0.14)	0.06 (0.13)

in all tasks when the tolerance boundaries were expanded to ±12 samples (<0.094s).

C. Influence of Threshold Value and Noise

Removing the amplitude threshold, without changing the proposed temporal threshold, had no effect on any performance measure under each walking condition (Table II). When the temporal threshold was reduced to 0.2τ, IC sensitivity was unaffected while precision decreased substantially due to misclassifying FCs as ICs (false positives). Conversely, when the temporal threshold increased to 1.2τ, IC sensitivity reduced substantially (0.47) while precision was only less affected (Table II-1). In this case, the increased temporal threshold extended the inter-peak distance beyond sequential ICs such that approximately every second peak went undetected, reducing sensitivity by ~50%. While the amplitude threshold had no effect on algorithm performance with the proposed temporal threshold, increasing the amplitude threshold markedly improved IC precision when the temporal threshold

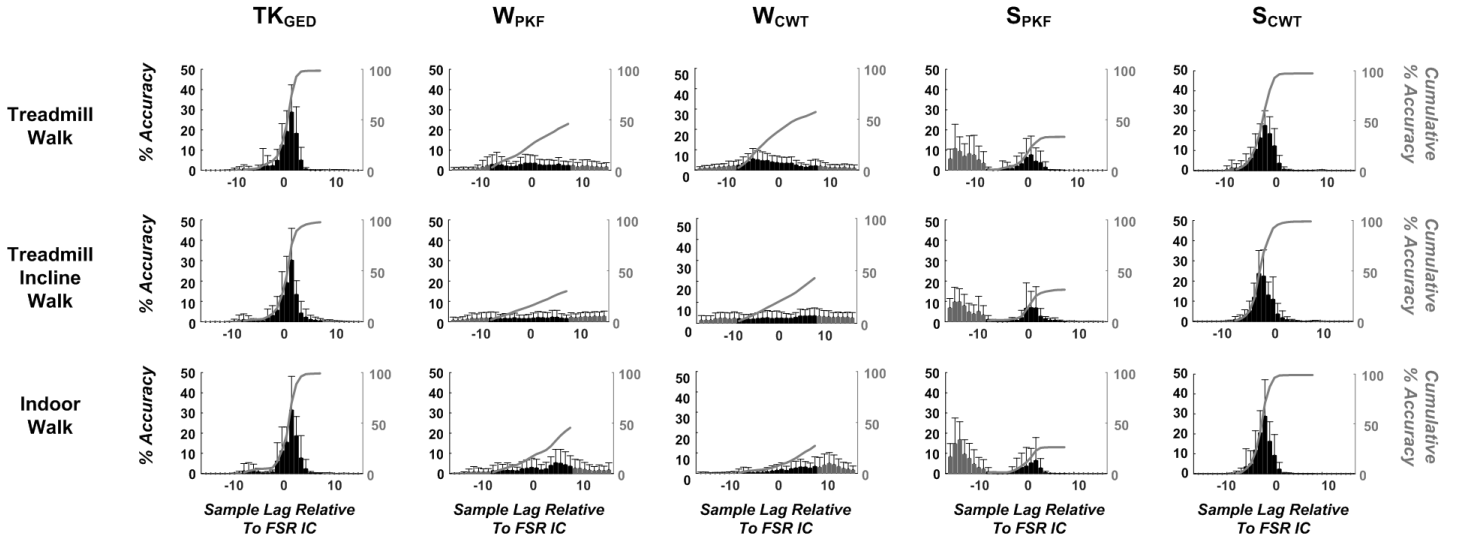

Figure 4. Distribution of IC estimates relative to the FSR approximated IC. The black bars represent the percentage of IC estimates occurring within the 8 sample tolerance of the FSR approximated IC, the grey bars show the percentage of estimates occurring outside the tolerance, and the grey curve represents the cumulative sum of the percentage accuracy at each sample between the tolerance boundaries. Shank based methods TK_{GED}, S_{PKF} and S_{CWT} show IC estimates in unimodal distributions close to zero, whereas W_{PKF} and W_{CWT} estimated are distributed more uniformly.

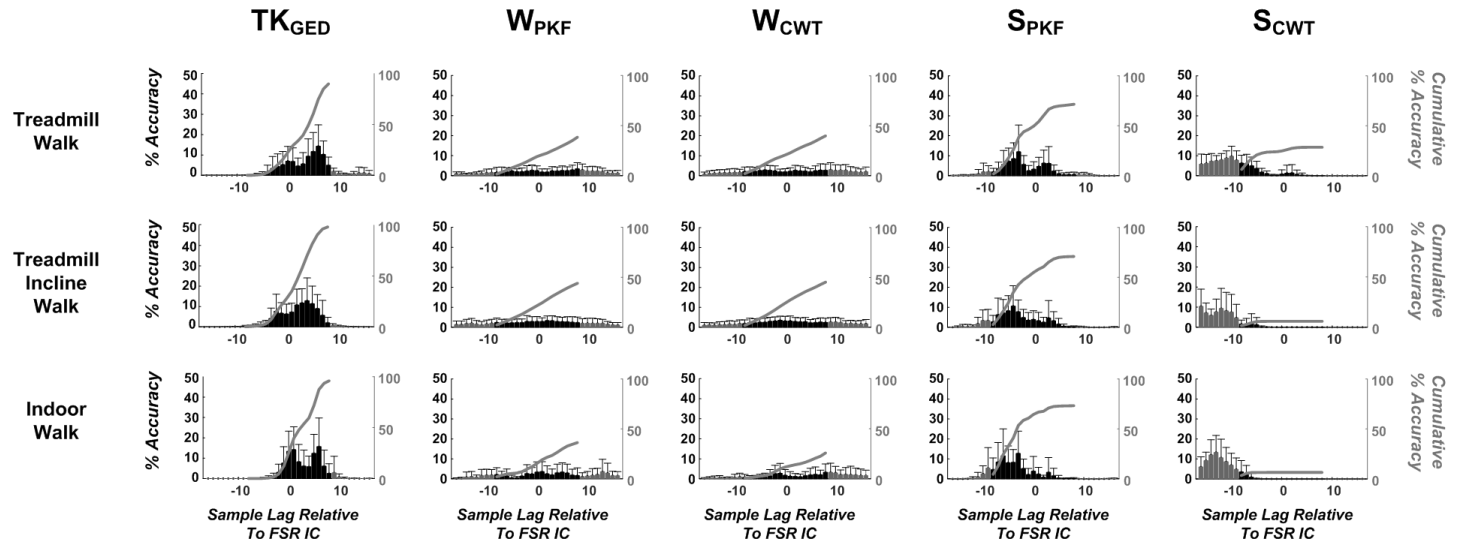

Figure 5. Distribution of FC estimates relative to the FSR approximated FC. The black bars represent the percentage of estimated occurring within the 8 sample tolerance of the FSR approximated FC, the grey bars show the percentage of FC estimates occurring outside the tolerance, and the grey curve represents the cumulative sum of the percentage accuracy at each sample between the tolerance boundaries. TK_{GED} is the only method to obtain detection accuracy >0.9 in walking tasks.

This article has been accepted for publication in a future issue of this journal, but has not been fully edited. Content may change prior to final publication. Citation information: DOI 10.1109/TBME.2019.2919394, IEEE Transactions on Biomedical Engineering

Table II.
The effect of the amplitude and threshold scaling factors on the mean (SD) sensitivity, precision and F1-score of ICs (1) and FCs (2) detected by TK_{GED} under all walking conditions. Rows with the proposed temporal threshold scaling factor (0.7τ), and columns with the proposed amplitude threshold (0.5 * TKO signal mean) scaling factor are shaded in light grey. Sensitivity, precision, and F1-score of TK_{GED} with the combination of proposed thresholds are shaded in dark grey.

1

			Sensitivity			Precision			F1 - score		
			Amplitude Threshold Scaling Factor			Amplitude Threshold Scaling Factor			Amplitude Threshold Scaling Factor		
			0	*0.5*	*1*	*0*	*0.5*	*1*	*0*	*0.5*	*1*
Treadmill (Flat) Walk	Temporal Threshold Scaling Factor	*0.2*	0.99 (0.03)	0.99 (0.03)	0.99 (0.03)	0.29 (0.02)	0.67 (0.11)	0.86 (0.12)	0.44 (0.02)	0.79 (0.09)	0.92 (0.08)
		0.7	0.99 (0.03)	0.99 (0.03)	0.99 (0.03)	0.99 (0.03)	0.99 (0.03)	0.99 (0.03)	0.99 (0.03)	0.99 (0.03)	0.99 (0.03)
		1.2	0.47 (0.05)	0.47 (0.05)	0.47 (0.05)	0.79 (0.04)	0.86 (0.06)	0.94 (0.06)	0.59 (0.05)	0.61 (0.05)	0.63 (0.05)
Treadmill (Incline) Walk	Temporal Threshold Scaling Factor	*0.2*	0.98 (0.04)	0.98 (0.04)	0.98 (0.04)	0.3 (0.02)	0.65 (0.14)	0.85 (0.16)	0.46 (0.03)	0.78 (0.11)	0.91 (0.12)
		0.7	0.98 (0.04)	0.98 (0.04)	0.98 (0.04)	0.98 (0.04)	0.98 (0.04)	0.98 (0.04)	0.98 (0.04)	0.98 (0.04)	0.98 (0.04)
		1.2	0.43 (0.02)	0.43 (0.02)	0.43 (0.02)	0.75 (0.03)	0.85 (0.09)	0.93 (0.09)	0.55 (0.02)	0.57 (0.03)	0.59 (0.03)
Indoor Walk	Temporal Threshold Scaling Factor	*0.2*	0.99 (0.01)	0.99 (0.01)	0.99 (0.01)	0.3 (0.02)	0.68 (0.14)	0.91 (0.14)	0.46 (0.02)	0.8 (0.1)	0.94 (0.1)
		0.7	0.99 (0.01)	0.99 (0.01)	0.99 (0.01)	0.99 (0.01)	0.99 (0.01)	0.99 (0.01)	0.99 (0.01)	0.99 (0.01)	0.99 (0.01)
		1.2	0.43 (0.01)	0.43 (0.01)	0.43 (0.01)	0.75 (0.03)	0.87 (0.07)	0.96 (0.08)	0.55 (0.02)	0.57 (0.02)	0.59 (0.02)

2

			Sensitivity			Precision			F1 - score		
			Amplitude Threshold Scaling Factor			Amplitude Threshold Scaling Factor			Amplitude Threshold Scaling Factor		
			0	*0.5*	*1*	*0*	*0.5*	*1*	*0*	*0.5*	*1*
Treadmill (Flat) Walk	Temporal Threshold Scaling Factor	*0.2*	0 (0)	0.41 (0.21)	0.74 (0.21)	0 (0)	0.51 (0.21)	0.79 (0.16)	0 (0)	0.45 (0.21)	0.76 (0.18)
		0.7	0.9 (0.15)	0.9 (0.15)	0.9 (0.15)	0.9 (0.15)	0.9 (0.15)	0.9 (0.15)	0.9 (0.15)	0.9 (0.15)	0.9 (0.15)
		1.2	0.15 (0.04)	0.15 (0.04)	0.15 (0.04)	0.25 (0.06)	0.25 (0.06)	0.25 (0.06)	0.19 (0.05)	0.19 (0.05)	0.19 (0.05)
Treadmill (Incline) Walk	Temporal Threshold Scaling Factor	*0.2*	0 (0)	0.42 (0.29)	0.8 (0.24)	0 (0)	0.51 (0.32)	0.86 (0.14)	0 (0)	0.45 (0.31)	0.82 (0.21)
		0.7	0.98 (0.02)	0.98 (0.02)	0.98 (0.02)	0.98 (0.02)	0.98 (0.02)	0.98 (0.02)	0.98 (0.02)	0.98 (0.02)	0.98 (0.02)
		1.2	0.12 (0.01)	0.11 (0.01)	0.11 (0.01)	0.21 (0.02)	0.21 (0.02)	0.21 (0.02)	0.15 (0.01)	0.15 (0.01)	0.15 (0.01)
Indoor Walk	Temporal Threshold Scaling Factor	*0.2*	0 (0)	0.43 (0.26)	0.83 (0.26)	0 (0)	0.6 (0.3)	0.84 (0.25)	0 (0)	0.49 (0.27)	0.84 (0.26)
		0.7	0.96 (0.11)	0.96 (0.11)	0.96 (0.11)	0.96 (0.11)	0.96 (0.11)	0.96 (0.11)	0.96 (0.11)	0.96 (0.11)	0.96 (0.11)
		1.2	0.12 (0.02)	0.12 (0.02)	0.12 (0.02)	0.21 (0.03)	0.21 (0.03)	0.21 (0.03)	0.15 (0.02)	0.15 (0.02)	0.15 (0.02)

increased/decreased (Table II-1). As FC detection relies on the prior detection of adjacent IC events, a combined reduction in IC sensitivity and precision substantially reduced FC detection accuracy (Table II-2).

At SNRs as low as 5dB, TK_{GED} detected IC events with consistently high accuracy under all walking conditions, with minimal reduction in sensitivity or precision values (F1-score = >0.97). FC detection accuracy remained relatively high at SNR levels up to 15dB (F1-score = >0.85). Despite moderate reductions in sensitivity and precision at an SNR level of 5dB, TK_{GED} FC detection accuracy remained high compared to all other methods without added noise (F1-score = >0.57).

IV. Discussion

The instantaneous change of shank velocity upon IC and FC during gait is manifested as a localised simultaneous increase in amplitude and frequency of the shank acceleration signal. Taking advantage of this property, it is possible to detect gait events under a large variety of walking conditions. However, to do so requires a method capable of efficiently capturing simultaneous amplitude and frequency changes of the ACC signal, such as the Teager-Kaiser Energy Operator. The TKO has been employed to analyse signals in many diverse applications [26]–[31], but until now its capacity to detect gait events from ACC has not been investigated.

Employing the TKO to detect ICs and FCs in walking tasks designed to capture variations of gait speed and inclination, the performance of the proposed TK_{GED} method was evaluated using mean absolute error, sensitivity, precision, and F1-scores. TK_{GED} ranked highest for IC detection across all walking conditions, achieving comparable accuracy with S_{CWT} (F1-scores >0.98). This exceeded the accuracy of other established GED methods using waist-mounted ACC (F1-scores <0.52) and shank-mounted ACC employing peak detection (F1-score <0.28). TK_{GED} was the only method to provide consistently high accuracy for FC detection as well as IC detection in all walking conditions (F1-score >0.9). FC detection accuracy was considerably lower for both shank-based and both waist-based methods examined, yielding maximum F1-scores of 0.71 and 0.44 respectively.

A difference in the distribution of gait events across the algorithms assessed was also observed, Figs. 2 - 5. Examining the distribution of estimated event times provides an additional insight not available from the mean error or mean absolute error which are typically reported with these algorithms [10], [14], [17]–[19]. ICs estimated using shank-based methods tended to

form a unimodal distribution with a defined peak, either leading or lagging the FSR estimated IC. In contrast, estimated events from waist-based methods were more uniformly distributed about the FSR estimated event, indicative of randomly distributed error. This outcome supports the results of previous studies that report poorer GED performance in methods for waist-mounted ACC than for shank-mounted ACC [10], [19]. Estimated ICs from TK_{GED} had distributions lagging the FSR approximated IC with mean errors of 8.89ms, 9.92ms, and 11.11ms for flat treadmill, incline treadmill, and flat indoor walking respectively. Similarly, the mean error for the distribution of estimated FC times were 33.04ms, 18.62ms, and 23.88ms in each walking condition. These mean errors reflect offsets relative to FSR estimated gait events, comparable with those reported previously [3], [10], [19]. Gait events detected by TK_{GED} (Figs. 2-3) occurred at times corresponding to peaks in the TKE signal that represent maximal simultaneous changes in amplitude and frequency (Fig. 1b). The shift of detected events relative to the FSR may partially be a consequence of the accelerometer position, or relate to differences in the nature of the accelerometer and force sensor signals. TK_{GED} ICs and FCs were also narrowly distributed about the FSR event in comparison to the other methods examined (Figs. 4-5), providing lower mean absolute errors which should yield more consistent estimates of gait cycle parameters.

While IC sensitivity was unaffected by reductions in the amplitude threshold (for temporal threshold = 0.7τ), precision declined substantially due to increased false positive detection, Table II-1. Precision increased at the higher amplitude threshold, but moderately declined as the temporal threshold value increased. These findings suggest that for steady-state gate, temporal thresholds lying between average step and stride time may be considered optimal, and may potentially obviate the amplitude threshold. Whereas, for applications involving more varied gait, the amplitude threshold becomes important for minimizing false positive ICs. Any reduction in IC sensitivity or precision will reduce FC detection accuracy. Collectively, these results demonstrate that employing the TK_{GED} method under irregular gait conditions with non-stationary stride time may require windowed or adaptive thresholding to achieve sustained accuracy.

The findings of the SNR analysis highlight the advantages of employing the TKO for gait event detection in the presence of noise. Up to SNR levels of 5dB, IC detection was mostly unaffected, while FC detection remained robust up to an SNR level of 15dB. In contrast to peak finding methods, these results indicate that low-amplitude noise distortion of the ACC signal profile will have a negligible impact on TK_{GED} performance, suiting its application in environments outside the clinic. Furthermore, TK_{GED} offers a method potentially suitable for detecting gait events in individuals with asymmetric gait profiles, as instances of IC and FC are detected for each leg independently. Compared to other methods, TK_{GED} does not rely quasi-constant or even step times between legs, nor on the order of a classic gait cycle profile, enabling left and right leg gait events to be captured separately. While developed and tested using ACC recorded from control subjects with regular, natural gait cycle profiles, further work is required to evaluate the suitability of TK_{GED} for pathological gait analysis, where gait asymmetry and irregularity are increased.

V. Conclusion

Whether to monitor altered walking patterns in the presence of disease [3]–[5], or to track patient mobility with rehabilitation [6], [7], accurate evaluation of temporal gait parameters is heavily dependent on precise IC and FC detection. Although many methods for ACC-based GED have been reported, the performance of these algorithms has been shown to vary greatly [19]–[21], with many dependent on specific signal profiles, cadence, or gait regularity.

To address this, a new method, TK_{GED}, is proposed to identify IC and FC times under various walking conditions with limited preconditions. By exploiting the amplitude and frequency sensitivity of the TKO, TK_{GED} can be implemented with relative simplicity without the need for signal pre-processing. The high accuracy of the method demonstrated here, highlights the effectiveness of the TKO for robust automated GED using ACC in a variety of walking conditions. Together, these features support the potential of TK_{GED} for real-time analysis of real-world gait data.

References

[1] K. M. Culhane, *et al.*, (2005, Nov) 'Accelerometers in rehabilitation medicine for older adults', *Age Ageing*, vol. 34, no. 6, pp. 556–560

[2] W. Tao, *et al.*, (2012, Feb) 'Gait analysis using wearable sensors', *Sensors*, vol. 12, no. 2, pp. 2255–2283

[3] J. Han, *et al.*, (2009, Aug) 'Adaptive windowing for gait phase discrimination in Parkinsonian gait using 3-axis acceleration signals', *Med. Biol. Eng. Comput.*, vol. 47, no. 11, pp. 1155–1164

[4] A. Salarian *et al.*, (2004, Aug) 'Gait assessment in Parkinson's disease: Toward an ambulatory system for long-term monitoring', *IEEE Trans. Biomed. Eng.*, vol. 51, no. 8, pp. 1434–1443

[5] S. Del Din, A. Godfrey, and L. Rochester, (2016, May) 'Validation of an Accelerometer to Quantify a Comprehensive Battery of Gait Characteristics in Healthy Older Adults and Parkinson's Disease: Toward Clinical and at Home Use', *IEEE J. Biomed. Heal. Informatics*, vol. 20, no. 3, pp. 838–847

[6] K. Turcot, *et al.*, (2008, Apr) 'New accelerometric method to discriminate between asymptomatic subjects and patients with medial knee osteoarthritis during 3-D gait', *IEEE Trans. Biomed. Eng.*, vol. 55, no. 4, pp. 1415–1422.

[7] C. A. Clermont and J. M. Barden, (2016, Oct) 'Accelerometer-based determination of gait variability in older adults with knee osteoarthritis', *Gait Posture*, vol. 50, pp. 126–130

[8] E. C. Wentink, *et al.*, (2014, Jan) 'Detection of the onset of gait initiation using kinematic sensors and EMG in transfemoral amputees', *Gait Posture*, vol. 39, no. 1, pp. 391–396

[9] A. Tura, *et al.*, (2010, Jan) 'Gait symmetry and regularity in transfemoral amputees assessed by trunk accelerations', *J. Neuroeng. Rehabil.*, vol. 7, no. 1, p. 4

[10] F. A. Storm, C. J. Buckley, and C. Mazzà, (2016, Oct) 'Gait event detection in laboratory and real life settings: Accuracy of ankle and waist sensor based methods', *Gait Posture*, vol. 50, pp. 42–46

[11] J. McCamley, *et al.*, (2012, Jun) 'An enhanced estimate of initial contact and final contact instants of time using lower trunk inertial sensor data', *Gait Posture*, vol. 36, no. 2, pp. 316–318

[12] S. Khandelwal and N. Wickström, (2016, Dec) 'Gait Event Detection in Real-World Environment for Long-Term Applications:

Incorporating Domain Knowledge Into Time-Frequency Analysis', *IEEE Trans. Neural Syst. Rehabil. Eng.*, vol. 24, no. 12, pp. 1363–1372.

[13] E. Sejdić, *et al.*, (2016, Dec) 'Extraction of Stride Events from Gait Accelerometry during Treadmill Walking', *IEEE J. Transl. Eng. Heal. Med.*, vol. 4

[14] R. W. Selles, *et al.*, (2005, Mar) 'Automated estimation of initial and terminal contact timing using accelerometers; development and validation in transtibial amputees and controls', *IEEE Trans. Neural Syst. Rehabil. Eng.*, vol. 13, no. 1, pp. 81–88

[15] A. Köse, A. Cereatti, and U. Della Croce, (2012, Feb) 'Bilateral step length estimation using a single inertial measurement unit attached to the pelvis', *J. Neuroeng. Rehabil.*, vol. 9, no. 1, p. 9

[16] H. K. Lee, *et al.*, (2009, Sep) 'Novel algorithm for the hemiplegic gait evaluation using a single 3-axis accelerometer', in *Proceedings of the 31st Annual International Conference of the IEEE Engineering in Medicine and Biology Society*, pp. 3964–3966.

[17] R. C. González, *et al.*, (2010, Mar) 'Real-time gait event detection for normal subjects from lower trunk accelerations', *Gait Posture*, vol. 31, no. 3, pp. 322–325

[18] D. Trojaniello, A. Cereatti, and U. Della Croce, (2014, Sep) 'Accuracy, sensitivity and robustness of five different methods for the estimation of gait temporal parameters using a single inertial sensor mounted on the lower trunk', *Gait Posture*, vol. 40, no. 4, pp. 487–492

[19] G. Pacini Panebianco, *et al.*, (2018, Oct) 'Analysis of the performance of 17 algorithms from a systematic review: Influence of sensor position, analysed variable and computational approach in gait timing estimation from IMU measurements', *Gait Posture*, vol. 66, pp. 76–82

[20] W. Zijlstra and A. L. Hof, (2003, Oct) 'Assessment of spatio-temporal gait parameters from trunk accelerations during human walking', *Gait Posture*, vol. 18, no. 2, pp. 1–10

[21] S. H. Shin and C. G. Park, (2011, Nov) 'Adaptive step length estimation algorithm using optimal parameters and movement status awareness', *Med. Eng. Phys.*, vol. 33, no. 9, pp. 1064–1071

[22] S. L. Murphy, (2009, Feb) 'Review of physical activity measurement using accelerometers in older adults: Considerations for research design and conduct', *Prev. Med. (Baltim).*, vol. 48, no. 2, pp. 108–114

[23] S. Patel, D. A. Asch, and K. G. Volpp, (2015, Feb) 'Wearable devices as facilitators, not drivers, of health behavior change', *JAMA - J. Am. Med. Assoc.*, vol. 313, no. 5, pp. 459–460

[24] S. Del Din, *et al.*, (2016, Sep) 'Measuring gait with an accelerometer-based wearable: Influence of device location, testing protocol and age', *Physiol. Meas.*, vol. 37, no. 10, pp. 1785–1797

[25] S. R. Simon, (2004, Dec) 'Quantification of human motion: Gait analysis - Benefits and limitations to its application to clinical problems', *J. Biomech.*, vol. 37, no. 12, pp. 1869–1880

[26] H. M. Teager and S. M. Teager, (1983) 'A Phenomenological Model for Vowel Production in the Vocal Tract', *Speech Sci. Recent Adv.*, pp. 73–109

[27] H. M. Teager and S. M. Teager, (1990) 'Evidence for Nonlinear Sound Production Mechanisms in the Vocal Tract', in *Speech Production and Speech Modelling*, Dordrecht: Springer Netherlands, pp. 241–261.

[28] J. F. Kaiser, (1990, Apr) 'On a simple algorithm to calculate the "energy" of a signal', in *International Conference on Acoustics, Speech, and Signal Processing*, pp. 381–384.

[29] X. Li, P. Zhou, and A. S. Aruin, (2007, Aug) 'Teager-kaiser energy operation of surface EMG improves muscle activity onset detection', *Ann. Biomed. Eng.*, vol. 35, no. 9, pp. 1532–1538

[30] V. Kandia and Y. Stylianou, (2006, Nov) 'Detection of sperm whale clicks based on the Teager-Kaiser energy operator', *Appl. Acoust.*, vol. 67, no. 11–12, pp. 1144–1163

[31] P. E. Caicedo, *et al.*, (2018, Oct) 'Gait Phase Detection for Lower Limb Prosthetic Devices', in *International Symposium on Wearable Robotics*, pp. 201–205

[32] P. Maragos, T. F. Quatieri, and J. F. Kaiser, (1993, Apr) 'On Amplitude and Frequency Demodulation Using Energy Operators', *IEEE Trans. Signal Process.*, vol. 41, no. 4, pp. 1532–1550

[33] S. Khandelwal and N. Wickström, (2017, Jan) 'Evaluation of the performance of accelerometer-based gait event detection algorithms in different real-world scenarios using the MAREA gait database', *Gait Posture*, vol. 51, pp. 84–90.

[34] N. Chinchor, (1992, Jun) 'MUC-4 evaluation metrics', in *Proceedings of the 4th conference on Message understanding - MUC4 '92*, p. 22.